OPEN ACCESS

International
Journal
Of Modern Engineering Research (IJMER)

Characterisation and Modeling of Precipitation Kinetics in 7075 Al-Zn-Mg Alloy

P.K. Mandal
Department of Metallurgical & Materials Engineering, Indian Institute of Technology Roorkee (IITR), Roorkee, UK-247667, INDIA

ABSTRACT:-*The precipitation kinetics in 7075 Al-Zn-Mg alloy have been investigated by age-hardening measurements and TEM, SEM, FESEM, and DSC characterization. The several ageing heat treatments were done at 120 ^{o}C, 140 ^{o}C and 180 ^{o}C. The tensile properties and fracture toughness property also revealed precipitation kinetics mechanisms at as-cast aluminium alloy. The present paper, the basic understanding to different precipitation sequences revealed through different ageing temperatures, as-well-as minor addition of transition element (e.g. Sc) activity during ageing kinetics speed up. It has been possible to achieve an ideal combination of strength, density, and thermal stability because of the unique precipitation-hardening characteristics of scandium (Sc). Moreover, the composition of the alloy is an important factor. In particularly, the Zn:Mg ratio has a pronounced effect on the mechanical properties that is ascribed to its influence on the precipitation kinetics. In this paper the effects of Zn and Mg variations with different Zn:Mg ratio on the precipitation behaviour of Al-Zn-Mg alloy at various heat treatment temperatures will be studied. The mechanical and physical properties of the age-hardening alloys will be modelled and presented.*

Keywords*:- age-hardening, fracture toughness, mechanical properties, precipitation kinetics, TEM, transition element.*

I. INTRODUCTION

Traditionally, 7075 Al alloy has found superior age hardening response in all aluminium alloys. It is well known that the alloys based on Al-Zn-Mg system are very important from commercial point of viewbecause of their high strength. They in fact widely used in automotive industry as well as structural application [1-8]. Applications to aluminium alloys for aero-structures have been described by Staley et al. [9]. An aluminium alloy product is usually selected based on its ability to provide the lightest and least costly structure. Specific strength is an important consideration as well as durability and damage tolerance in a number of forms. Resistance to catastrophic failure due to the presence of flaws (toughness), subcritical crack growth from cyclic loading (fatigue crack propagation), or environmental interactions (stress corrosion), among others, are important factors in the design of aircraft structure [10]. Improvements in aluminium alloys for aerospace applications during the past few decades have been associated with an improved understanding of the relationships among composition, processing, microstructure and properties. A lot of effort has been spent on investigation of the precipitation process in Al-Zn-Mg alloys. There has been considerable interest in the modelling of precipitation kinetics and strengthening in age hardening 7075 aluminium alloys. If these aluminium alloys contain small scandium additions present improved properties in several fields. Scandium, when added to aluminium alloys, is a powerful dispersoid strengthener, grain refiner and recrystallizationinhibitor. The Al_3Scdispersoid ($AuCu_3$-type phase) is coherent with the Al-matrix. It is well known that several transformation sequences may occur in these materials during ageing and that quenched-in vacancies play an essential role in the precipitation of ή phase. The equilibrium precipitates can form numerous crystallographic orientations with respect to matrix, and it has been found that the presence of dislocations can significantly alter the precipitation process. Nucleation of precipitates can occur more readily on dislocations, as the free-energy change required for nucleation can be substantially reduced and, also, the growth and coarsening of precipitates can be enhanced due to short-circuit diffusion along the dislocation core[11**]**. Particularly there are two alternative routes for ή formation: GP-I zones and vacancy rich clusters (VRC) zones, formed during quenching to room temperature after solution treatment. Vacancy rich cluster are thought to be formed either after or during quenching to room temperature, to be quite stable at this temperature and constitute the main formation route to ή with GP-II zones as intermediate phase. At ageing temperature above GP solvus, GP-II transform into ή while GP-I either dissolves or transform into ή if it has reached some critical size. The value of

strength obtained by precipitation process depends on solution and hardening temperature, deformation prior to ageing and additional ageing elements. The temperature of artificial ageing influences the kinetics and the sequence of precipitation and if heterogeneous nucleation of the equilibrium phase appears, a less hardening is obtained. In this study, one solution temperature (at 465 ^{o}C) has been considered and the response to several artificial ageing treatments analyzed in the range of 120 to 180 ^{o}C [12]. The precipitation sequence that is known to occur in the Al-Zn-Mg based alloys can be described as follows: Supersaturated solid solution→ GP (GP-I and GP-II) + VRC → ή phase→ η phase ($MgZn_2$). Guinier-Preston (GP) zones precipitate in many aged supersaturated alloys such as Al-Cu, Al-Zn, Al-Zn-Mg, and so on. It is found that GP zones precipitation is the essential reason for strengthening in alloys and it has much influence on the formation of the latter phase. In contrast, the GP zones to ή transition is of great importance both for the kinetics of precipitation and for the hardening behaviour [13]. In addition, the precipitation of GP zones is promoted by the increase of Zn or Mg content. The quantities of stable (η) and metastable (ή) phases have been calculated under various Zn and Mg contents by using software package JmatPro, it has adapted by J. Yu et al.[2011][14]. Scandium additions have also significantly changed precipitation kinetics in age hardening conditions and must be accounted for. However, at higher temperatures, the yield strength of 7075–T_6 rapidly decreases due to dissolution or transformation of the metastable phases (ή) into the equilibrium η phase. It is believed that the probability of the transformation occurring will depend upon the activation energy required for the transformation in the crystal structure. So, in the present cases likely multi-component systems Al-Zn-Mg and Al-Zn-Mg-Sc has led to low activation energies.There are several theoretical models have been discussed on precipitates kinetics mechanisms and correlation made with experimental works on studied alloys. It is worth noting that the present experimental results have been discussed in order to insight observation with theoretical models and from literatures supported on the precipitation behaviours of aluminium alloys are studied.

II. EXPERIMENTAL PROCEDURE

The Al-Zn-Mg alloys were melted in pure Al, pure Zn, and pure Mg with the addition of Al-2wt% Sc master alloyin electrical resistance muffle furnace at 780 ^{o}C. The chemical composition wasanalyzed by ICP-AES(inductively coupled plasma atomic emission spectroscopy) of studied alloys (in wt %) as presented in Table-1. The cast alloy was preferred for solution treatment at 465 ^{o}C for one hour then immediately water quenching (e.g. it designated asT_4 heat-treatment) and subsequently artificial ageing treatments were performed for predetermined three temperatures at 120 ^{o}C, 140^{o}C and 180 ^{o}C (e.g. each temperature designated as T_6 heat-treatment), respectively. During each artificial ageing treatment hardness (generally average of five indentations of each hardness selected) was tabulated through Vicker's hardness (FIE-VM50 PC) measurement with specific load at different time interval up to sixteen hours.The cast samples for metallographic observation were prepared through a conventional mechanical polishing and followed by etching with modified Keller's reagent solution(2.5 ml HNO_3+1.5 ml HCl+1 ml HF+ 95 ml water). The cast alloys were examined under optical microscope to findings grain size (in µm), grain boundary segregation (in volume% second phases), and porosity contents (in volume%).The cast alloys were gone through metallographic examinations and several characterizations were performed through OM (optical microscopy), EPMA (electron probe micro analysis), SEM (scanning electron microscopy), FESEM (field emission scanning electron microscopy), TEM (transmission electron microscopy) and DSC (differential scanning calorimerty) analysis. The tensile tests were carried out by using an Instron tensile testing machine (e.g. cross head speed of 1 mm/min, 25 mm gauge length and 5 mm gauge diameter). The tensile test samples were collected from as-cast alloy as well as after T_6 (e.g. solutionized from 465 ^{o}C for one hour then immediate water quenching plus aged 160 ^{o}C two hour) heat-treated alloys. Consequently, the fracture toughness test was conducted by Instron Universal testing machine (Model no.: 1342) with standard (ASTM E399) CT specimen with static loading condition.

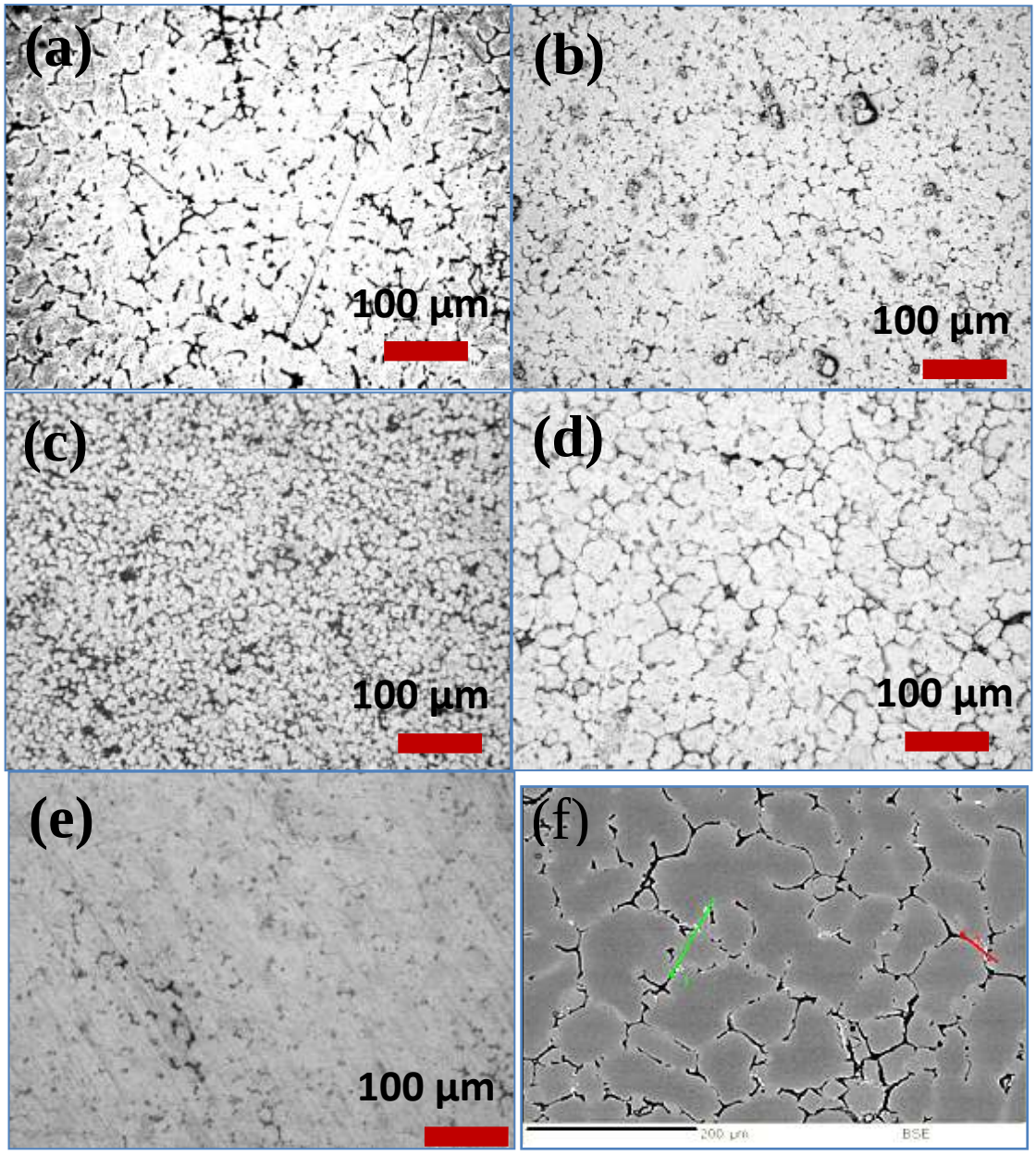

Fig.-1: Illustration of optical micrographs of as-cast alloys: (a) Alloy-1, (b) Alloy-2, (c) Alloy-3; T_4 micrographs of (d) Alloy-2, (e) Alloy-3; EPMA micrograph of (f) Alloy-1.

Table-1: Chemical composition of studied 7075 Al-Zn-Mg alloys (in wt %).

Alloy no.	Zn	Mg	Sc	Si	Fe	Al	Zn/Mg	Zn + Mg
1	6.65	2.80	-	0.03	0.01	Bal.	2.38	9.45
2	5.30	2.90	0.25	0.11	0.10	Bal.	1.83	8.20
3	5.10	2.80	0.33	0.12	0.14	Bal.	1.82	7.90

III. RESULTS AND DISCUSSION

The precipitation from a solid solution and the related hardening of Al-Zn-Mg alloys is one of the most investigated areas of physical and mechanical metallurgy, both from the experimental and the theoretical viewpoint. The Al-Zn-Mg alloys family provides some of the most interesting alloys for light-weight structural applications, where specific strength (strength-to-weight ratio) is a major design consideration, in particular in aircraft industry [15]. So far, the Al-Zn-Mg alloys have been highly used in aircraft industry for more than 80

years, and recent advances in aluminium alloy development maintain these alloys as the materials of choice for future commercial aircraft structures [16]. However, the decomposition stages are more important, which is depending on the details of the thermal treatments. The compositions of the alloys are an important factor to formation of leading phases during ageing kinetics. However, Boyd and Nicholson [1971] have found that at the beginning of ageing the growth of precipitates (during under-aged) followed a $t^{1/3}$ law but at over-aged stage followed a$t^{1/2}$ law. The composition of aluminium alloys is also a significant factor in controlling the aspect ratio of precipitates. It can be inferred from this equation f(A) = $\sqrt{A} - \frac{A_e}{\sqrt{A}} = \frac{\pi B}{9\gamma}\sqrt{\Omega Dt/p}$……(1); where A is the aspect ratio of precipitates, A_e is the equilibrium aspect ratio, B is the function of the elastic strain ε, γ is the precipitate-matrix interfacial energy, D is the diffusion coefficient of solute atom in solvent, t is the ageing time and Ω is related to β =Ω/pA , β is a dimensionless growth parameter and p being a factor of 2/3 value for continuous precipitation that higher nominal content of solute in solution will bring about more enough supersaturation and concomitant larger aspect ratio. This may be attributed to the ability for nucleation and growth of precipitates. When the nominal content of solute is lower, the drive force for nucleating precipitates is weaker, so less density is come out for precipitates and the excess solute atoms are adequate to meet the need for unlimited extension of habit plane of precipitates. Consequently, it could be seen that the aspect ratio of precipitates is as well changing during the ageing process in the aluminium alloys. According to Merle et al.[1981] and Sankaran et al. [1977, 1978] have pointed out that the aspect ratio of precipitates increase monotonously to a maximum value and where after decrease monotonously because the potential for growth of habit plane of precipitates is gradually exerted to the most extent. Once this potential being exhausted after prolonged ageing, the ability of growth of inherent plane is then coming cut a noticeable figure. From the equation-(1) hints that, the aspect ratio of plate-shaped precipitates is influenced not only by ageing time but also by diffusion coefficient and supersaturation. It is well known that the diffusion coefficient depends on ageing temperatures in exponentially direct proportion and the super saturation depends on ageing temperatures in exponentially reverse proportion, so the product of diffusion coefficient with supersaturation varies with ageing temperatures in a curve of saddle-shape. At lower ageing temperatures, the diffusion of solute atoms is slower which results in a less value for aspect ratio, although the drive force for growth is higher. But at the higher ageing temperatures, the aspect ratio is still low due to a smaller drive force and the readily occurred loss of coherency or semi-coherency of habit plane. The relatively larger value for aspect ratio is obtained at intermediate ageing temperature where both enough drive force for growth and enough ability for diffusion of solute atoms are contemporarily achieved [17]. The normal precipitation sequence during ageing of the supersaturated solid solution that is known to occur in the Al-Zn-Mg based alloys can be described as follows: Supersaturated solid solution→ GP (GP-I and GP-II) + VRC → ή phase→ η phase ($MgZn_2$). The decomposition reaction commences with the formation of GP zones, which eventually transform into metastable ή transition phases. The transition phases are more thermally stable than GP zones.In Fig.-2 shows a flow diagram of precipitation sequences in aluminium alloys. Results from experimental and numerical investigations obtained for either Al 7075 alloy or similar Al-Zn-Mg alloys suggest that the formation of GP zones is highly dependent

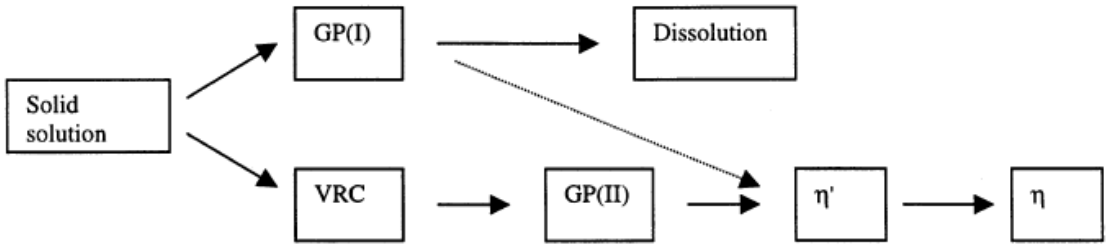

Fig.-2: The flow diagram of precipitation sequence in the Al-Zn-Mg alloys.

on the excess vacancy concentration. Hence, in a vacancy-depleted Al matrix, defects such as dislocations will become the major nucleation sites that promote heterogeneous nucleation. A numerous analysis has been done by T. Hu et al. on coarse grained and ultra-fine grained with deformed samples characterisation of Al 7075 and Al 7075-T_6. Our aim has to analyzed on theoretically and experimentally in precipitate-dislocation mechanisms on cast alloys but for better understanding purpose also consider as well as deformed alloys. So, on theoretical explanation as per T. Hu et al. based on the analysis, GP zones do not locate precisely of dislocation cores [18]. They have shown relationship on b = a$\sqrt{h^2 + k^2 + l^2/2}$ where b is the Burgers vector, a is the unit cell length. The radius for an edge dislocation core ranges in magnitude from b to 4b. Hence in the case of a dislocation along {111} planes in fcc Al, b values to 3.5A^o. Hence they have suggested that GP zones do not nucleate directly from the dislocation core but from a region very close to the dislocation core. In this case, segregation

of solute atoms and fast diffusion near dislocation cores will critically influence nucleation kinetics. In the present study, it is hypothesized that solute atoms on the substitutional sites, e.g. Zn, Mg etc, cause lattice distortion, which may be partially released if these solute atoms segregate near line defects to form a Cottrell atmosphere. Generally, oversized solute atoms (e.g. Mg atoms) segregate to the dilated part of the dislocations, which is near the dislocation core below the dislocation line, whereas undersized solute atoms (e.g. Zn atoms) are likely to migrate toward the compressed regions above the slip plane. This migration therefore leads to the segregation of solutes along dislocation lines and to the formation of solute-enriched regions. The nucleation of precipitates on dislocations begins with the interaction between solute atoms and dislocations. The interaction of vacancies and substitutional or interstitial impurities with dislocations leads to distortions in the surrounding crystal. The distortion may interact with the stress field of the dislocation to raise or lower the elastic strain energy of the crystal. There are two ways to move the solute atoms towards the dislocation. One is the stress field created by dislocations, which could be driving force for the migration of solute atoms. The other condition for the formation of these Cottrell atmospheres is that the temperature is sufficiently high for defect migration to occur but not so high that the entropy contribution to the free energy causes the atmosphere to evaporate into solution matrix. Hence, these dislocations will attract more solute atoms during solution treatment, with diffusion as the driving force, which will cause more solute atoms to be displaced into the Cottrell atmosphere. In addition to dislocation-induced segregation, dislocation cores also act as fast paths for diffusing atoms since disorder in the core region effectively lowers the activationenergy for diffusion. Eckert et al. [1993] and Schwarz [1998] also proposed that the energy surplus from the solid-core interactions and the relatively open structure of the cores causes the solutes to diffuse along the cores. In the case of nucleation of nanometer-sized precipitates, such as the ones in the present study, diffusion paths through dislocation cores are likely to be important and dominant. During the ageing treatment or slow cooling following deformation, vacancies, which are essential for nucleation, migrate towards dislocations, since vacancies are readily affected by the stress field caused by dislocations. Once the vacancies approach solute atoms in the Cottrell atmosphere around the dislocation cores, solute-vacancy clusters, e.g. Zn-vacancy clusters, Zn_2- vacancy clusters and Mg- vacancy clusters, thus form and grow into GP zones. Although Zn and Mg atoms take part early during cluster formation, the process is controlled by the diffusion of Mg atoms since the activation energy for the migration of a Mg-vacancy (~0.6 eV) is higher than that of a Zn-vacancy (~0.21 eV) and an Zn_2-vacancy (~0.42 eV). In related work, Monte Carlo simulations suggest that large clusters grow as solute atoms diffuse from the matrix. Consequently, the rapid depletion of matrix solute leaves a very low supersaturation of Mg and hence the growth will again be limited by the diffusion of Mg atoms. However, heterogeneous nucleation assisted by solute atoms in a Cottrell atmosphere and the rapid diffusion along the cores facilitate the Mg diffusion into the clusters, thereby facilitating the formation of GP zones and the more stable ή phase precipitates, as observed in fine grained and deformed samples Al7075 and Al7075-T_6. Since the nucleation was assisted by dislocations, it is reasonable to deduce that the efficiency of heterogeneous nucleation and growth of precipitates, e.g. GP zones and ή phase precipitates, is controlled by the dislocation density in the grain interior.In addition, they have reported for Al-Zn-Mg, solution heat-treating at 465 ^oC and ageing at 135 ^oC will result in a precipitate-free zone (PFZ) ~250 nm away from the grain boundary. In this regards on the brief discussion, a theoretical kinetic modelbased on the approach given by Cahn and Hilliard, was applied for a simulation of the formation and growth of GP zones in 2000 series of Al-Cu alloys [19]. The concentration of GP zones predicted by the present model is based on the equilibrium between GP zones and the surrounding matrix. The GP zones are supposed to be the Cu-enriched area with increasing value of diameter and one lattice constant in height. The middle layer of GP zones is mainly composed of Cu atoms, and the top and the bottom half-layers are Al atoms. From Fig.-3 it can be concluded that the equilibrium concentration of GP zones is less than 35 at.% Cu. This prediction on the scope of Cu content of GP zones agrees well with many other investigations. Similarly, is shown in Fig.-4 the analysis of quantities in the matrix composition and the GP zone radius are reasonable. As per thermodynamic model description the total energy of GP zones is theequal to the strain energy and the interfacial energy, the total Gibbs energy of one mole of atoms is $G_m^{GP} = G_m^{bas} + G_m^{str} + G_m^{int}$ …..(2). Form the equ.(2), G_m^{bas} is the molar Gibbs energy expression of GP zones without considering the strain energyG_m^{str} and the interfacial energy G_m^{int} between the matrix and the precipitates. The strain energy is a function of the composition of GP zones, the composition of the surrounding matrix, the radius of GP zones and the temperature. Taking into account the coherent interface between the matrix and GP zones and the influence on the elastic strain energy from the shape of precipitates, G_m^{str} is given as follows: $G_m^{str} = 4G\delta^2 V\nu$ ……(3), where G is the shear modulus of the matrix, δ the degree of misfit: $\delta = \frac{a_o - a}{a_o}$ with a_o and a the lattice constants of the matrix and GP zones respectively; V the volume of one mole of the matrix from which GP zones precipitate: $V = \frac{a_o^3 N_o}{4}$ supposing that the GP zone is a monolayer of the (100) plane coherent with the fcc matrix; and ν the shape coefficient of precipitates. According to Becker, the interface free energy is determined by the energy of bonds across the

interface. This implies that only pair interactions between nearest-neighbour atoms are taken into account, that a mean field approximation is applicable to interface, that all interface stress contributions to the Gibbs free energy of the crystal can be separated from the chemical distributions, and that entropy contributions are so small that they can be neglected. The interfacial energy γ of a plain interface can be given as $\gamma = Z_{int}\ (\Delta c)^2\ \varepsilon$……(4), where Z_{int} is the density of atomic bonds across a unit interface area, (Δc) is the concentration

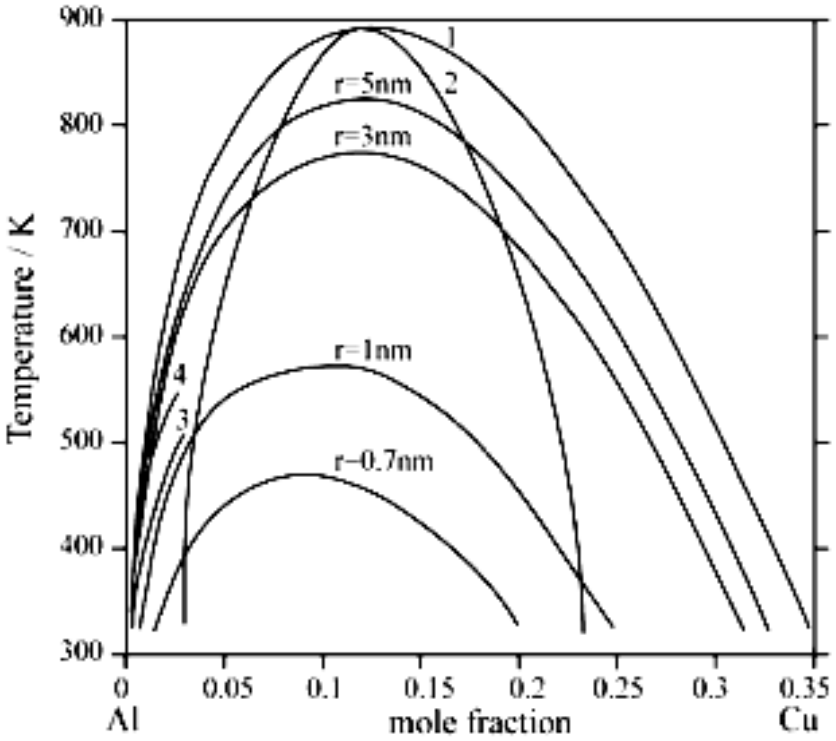

1- miscibility gap of fcc (Al); 2- spinodal decomposition of fcc(Al);3- GP solvus curve; 4- θ " solvus curve

Fig.-3: The equilibria between the matrix with various composition.

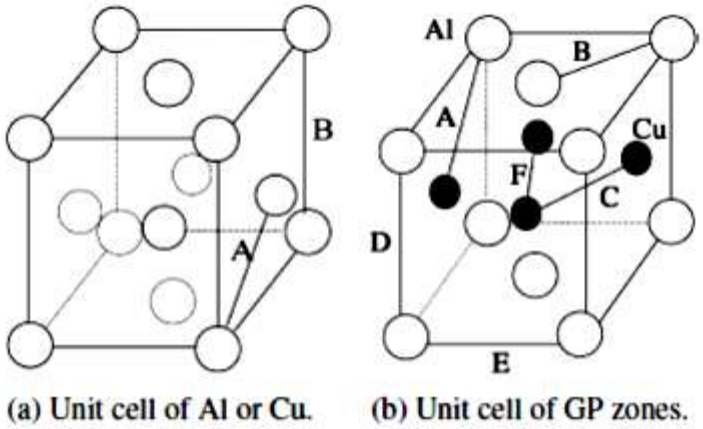

Fig.-4: Structure model showing the types of bonds.

difference across the interface, ε is thepair interaction energy. H. Yan-hui et al. [20]has been indicated in his paper on the modelling of precipitation kinetics is based on Kampmann and Wagner (KW) type numerical model, which has been used by several researchers. The model is based on homogeneous precipitation on Al alloys. They have explained on the activation energy for homogeneous nucleation consists of three parts, namely, the chemical free energy arising from the chemical supersaturation of the solutes, the interfacial energy spent for creating the precipitate/matrix interface and the strain energy used to accommodate the strain mismatch. The energy for nucleation, which is defined as the smallest activation energy barrier ΔG^*, is the energy for precipitates to reach the critical radius, the most effective way to minimize ΔG^* is to from nucleus, which has the minimum interfacial energy: $\Delta G^* = \frac{16}{3}\pi \frac{\gamma^3}{\Delta g^2}$……(5). The nucleation rate is calculated via the

classical Becker-Doring theory, and the precipitates density is given by the nucleation rate. The nucleation rate can be written as $\frac{dN}{dt}$= N_o $Z\beta^*$ exp($\frac{\Delta G^*}{KT}$)exp(- $\frac{\tau}{t}$) ……(6), where N is the precipitate density,$N_o$is the number of atoms by unit volume (=1/Vat.), t is the time, Z is Zeldovich's factor, K is the Boltzman constant,$\beta^* = 4\pi R^{*2} DC/a^4$, D is the diffusion coefficient of solute atoms in the matrix, and a is the lattice parameter of the precipitateN. Kemp et al. hints in his paper on the Kampmann and Wagner numerical model (KWN model). The model considers the nucleation, growth and coarsening/dissolution of the metastable and equilibrium precipitates phases, ή and η with their stochiometric composition, $MgZn_2$ [21]. In order to obtain improved mechanical properties, aluminium alloys are often subjected to different heat treatments. Generally, the solution treatmentis a primary and key step. During the solution treatment, the soluble phase formed during solidification can be re-dissolved into the matrix. At a higher solution temperature, the soluble phase can re-dissolved more sufficiently. However, for the single-stage solution treatment, the solution temperature must be below the incipient melting point for each specific composition. Otherwise, the alloy may be over burnt. The specimen treated with an enhanced solution exhibit a significant increase in the yield strength and fracture toughness because the residual phase can be re-dissolved into the matrix beyond the overburning temperature of the single-stage solution treatment. Usually, second phase particles is the void/crack sources or preferential crack paths and fracture toughness also marginally fall as the volume fracture of the second phase particlesincreases. With increasing the solution temperature, more and more second phase is dissolved, reducing the favourable nucleation sites for voids, which results in the increasing of the fracture toughness. Meanwhile, thesize of the sub-grains and the volume fraction of the recrystallized grains increase significantly with increasing

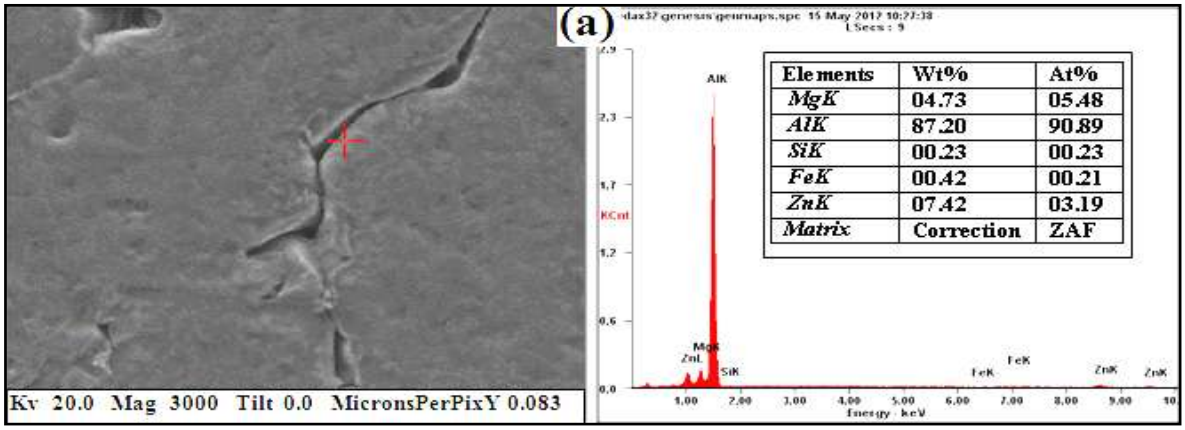

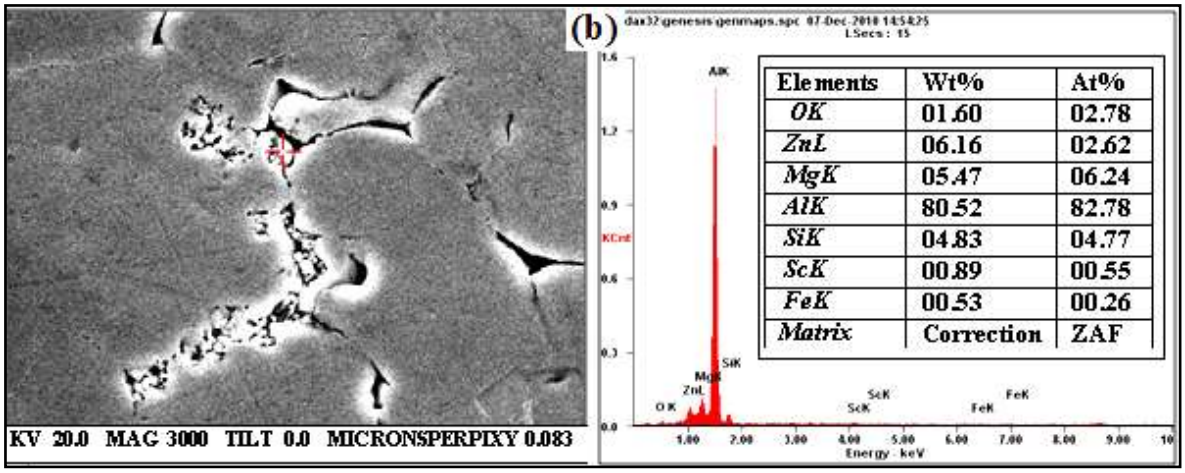

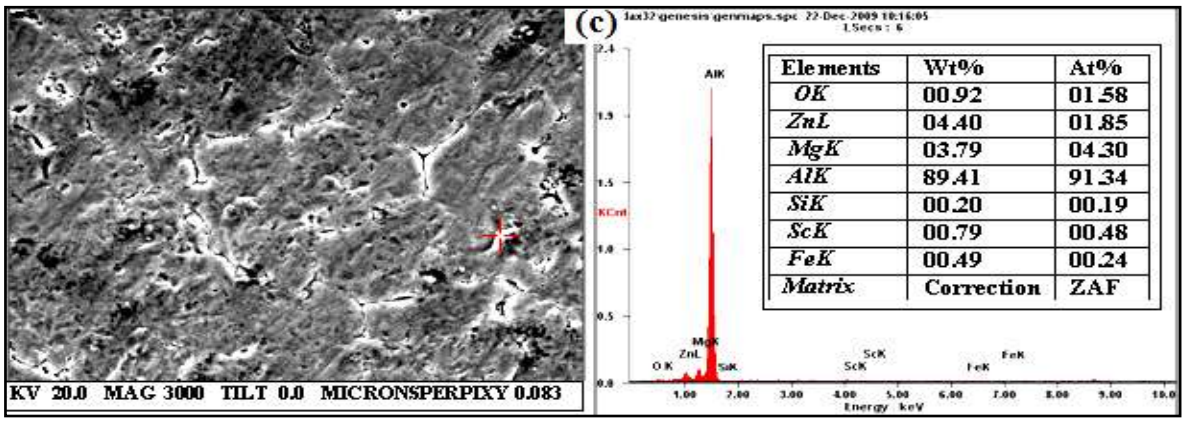

Fig.-5: FESEM micrographs with EDS analysis (as-cast): (a) Alloy-1, (b)Alloy-2, (c) Alloy-3.

the solution temperature which leads to a larger average grain size and the decreasing of the fracture toughness. Especially, the high angle grain boundaries of the recrystallized grains are the prefer propagation path for the crack and the fracture toughness decrease with increasing of the volume fraction of the recrystallized grains [22]. In this experimental study, one solution temperature (at 465 ^{o}C) has been considered and the response to several artificial ageing treatments analyzed in the range of 120 to 180 ^{o}C. This heat treatment is performed over a wide range of temperatures, usually several steps. The first step ranges from 100 to 120 ^{o}C which is within the stability range of GP zones, and the second step from 140to 170 ^{o}C which is the temperature range for ή and η precipitation and so on. In summary, Zn and Mg as the major alloying elements in Al-Zn-Mg alloy system play an important role in the formation of the precipitated phases in the alloys, especially for η($MgZn_2$) phase, and T($Al_2Mg_3Zn_3$) phase based on the assumption that thevaried elements acts alone without interactions with other alloying elements.The alloy with high Zn content may have good mechanical properties with more hardening phases ή and η precipitating after ageing treatment, whereas with high Mg content that the T and T'phase increase at the expense of η and ή phase, and the presence of T phase in the alloy largely depends on the Zn/Mg ratio. Therefore, when Zn/Mg ratio over two is formed η($MgZn_2$), with lower ratios formed T($Al_2Mg_3Zn_3$) [23, 24**]**. In addition, scandium to Al-Zn-Mg alloy accelerated ageing kinetics and concentrated GP zones formation. Moreover, scandium elements in Al-Zn-Mg alloy mainly exist as Al_3Sc particles. Primary Al_3Sc particles can refine the casting structures, which leads to fine grain. Secondary Al_3Sc particles can producesubstructure strengthening and precipitation strengthening. The optical micrographs of cast alloys have shown in Fig.-1(a-c). Coarsened as-cast grains, dendritic structures, segregation and eutectic formation on grain boundary observed in the Alloy-1. While, minor scandium (from 0.25-0.33%) addition can significantly refine gradually of the cast grains in the Alloy-2 and Alloy-3. In addition, the fine grain size achieved due to heterogeneous nucleation sites, Al_3Sc. In Fig.-1 (d-e) shows, solution treatment alloys exhibited that elimination of grain boundary segregation and dendrites, as well as cast inhomogeneties, eutectic phases reduces are observed. The EPMA spot analysis revealed grain boundary segregation of solute atoms in the as-cast alloy, shown in Fig.-1(f). In Fig.-5 (a-c) shows, FESEM with EDS analysis of as-cast alloys. This examination mainly exhibits grain boundary segregation of impurity elements. The Al-Zn-Mg alloys are very prone to grain boundary segregation and impair PFZ (precipitation free zone). In this task, three types of cast alloys are revealed mainly impurities elements like to Fe and Si, others. Scandium concentration more in grain boundary regions in as-cast condition can be observed during EDS analysis. The artificial ageing has been carried out to all three present alloys to following temperatures at 120 ^{o}C, 140 ^{o}C and 180 ^{o}C,respectively [Fig.-6(a-c)].During artificial ageing treatmentis to make strengthening phases precipitate from the supersaturated solid solution. The strengthening is associated with the shearing GP zones and ή phases by dislocation during deformation. In Fig.-6(a) shows Alloy-1 at 140 ^{o}C ageing phenomena highest hardening effect (at 10 kg. load) due to ή formation exhibiting more hardness in among three ageing temperatures, and this curve shows continuous flow of hardness in this temperature regime. In Fig.-6(b) shows similar trend to Alloy-2 at 140 ^{o}C ageing phenomena highest hardening effect (at 10 kg. load) due to ή formation and Al_3Sc particles effects exhibiting more hardness in among three ageing temperatures, but others two temperatures as hardening response not much effective due to coherent GP zones formation at 120 ^{o}C and equilibrium stable η phase formation at 180 ^{o}C. In Fig.-6(c) shows Alloy-3 in present three ageing temperatures are exhibiting similar hardening trend (at 10 kg. load), only at 180 ^{o}C showing slightly more hardness but all three curves are maintaining continuous flow in age hardening regime, it has concluded that at all three temperatures are fall in η-phase stable state with Al_3Sc particles effects just maintain continuous flow of curves even at longer ageing time. Therefore, hardness vs. ageing time curves exhibit three regions: (i) rapid increase in hardness (under-

ageing); (ii) plateau in hardness in curves (peak-ageing); (iii) decrease in hardness (over-ageing). This indicated that hardening from minor scandium was independent of hardening caused by other ageing precipitates in Al-Zn-Mg alloys [25].In Fig-7(a-b) shows that the as-cast TEM micrographs of 7075 alloys. They are minor scandium added, which have contributed uniform precipitates in fine grains matrix. Since both the alloys are as-cast feature then there precipitates formation are arbitrarily embedded on grain boundary for Alloy-2 (in Fig.-7.a), but for Alloy-3 (in Fig.-7.b) some cauliflower shape Al_3Sc particles observed in matrix. But both the alloys have fine grains matrix due to scandium grain refiner's contribution. In Fig.-7(c-d) shows that the morphology of precipitates uniformly distributed throughout the matrix of both the 7075 alloys, which have continues aged at 140 ^oC for 6 hours then room temperature cooling. The small round clusters are typically GP zones, whereas the fine platelet precipitates are the ή phase precipitates, which has indicated highest hardness peak during artificial ageing treatments in Fig.-6(a-b). At this stage ageing treatment usually called peak-aged regime,where GP transferredto ή-phase intermediate stage.

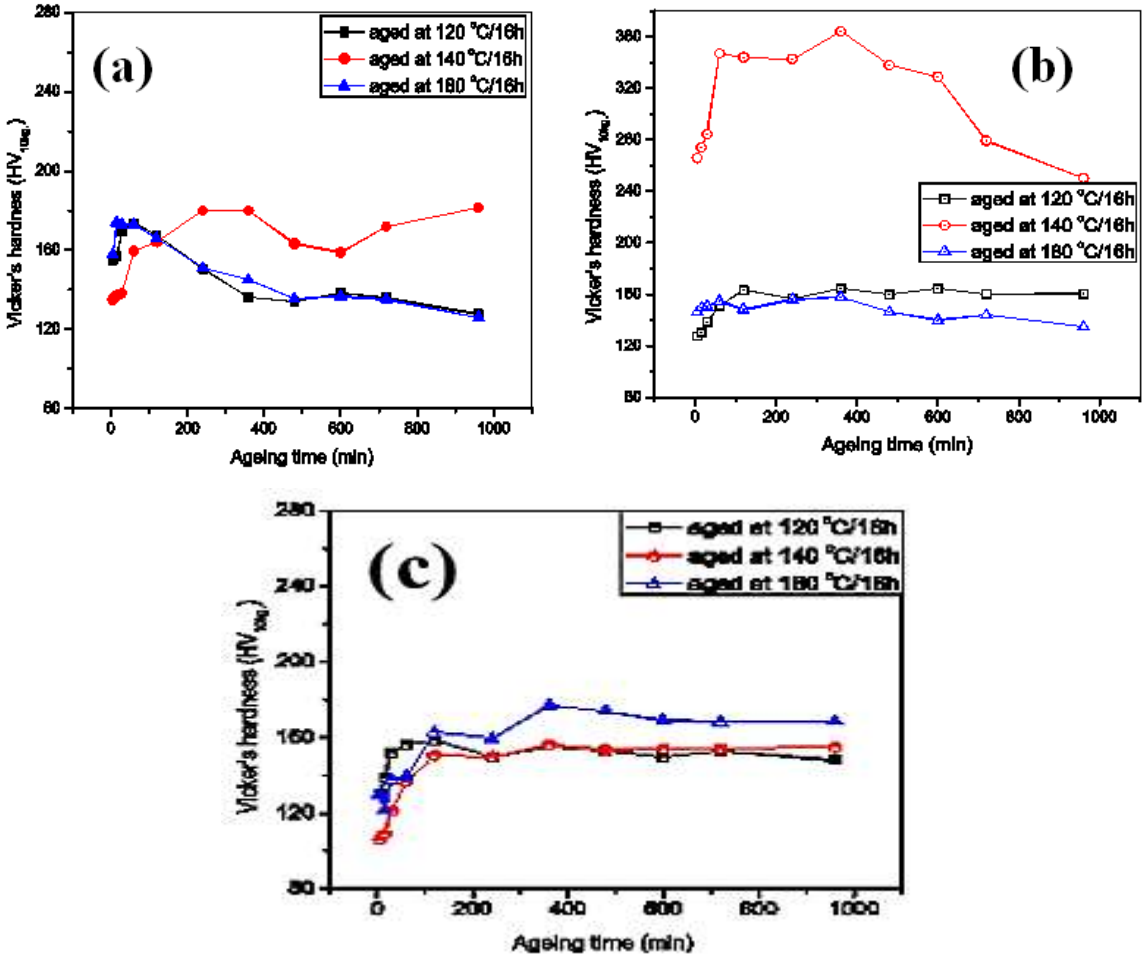

Fig.-6: Illustration of ageing curves at differenttemperatures: (a) Alloy-1;(b) Alloy-2; (c) Alloy-3.

Both GP zones and ή phase precipitates are uniformly distributed in the aluminium matrix. This suggests that the nucleation and growth of precipitates are predominately formed by homogeneous nucleation from a highly supersaturated solid solution and subsequently ageing treatment. On the other hand, for Alloy-2 (in Fig.-7.d) shows more dense and uniform distribution of precipitates and more numbers of platelet precipitates observed due to scandium addition to coherent Al_3Sc phase formation, which might be speed up the uniform precipitates.In this phenomena the activation energies (Q, kJ/mole)evaluation is more important parameter in the quantification of alloy age hardening behaviour in terms of activation energy of a precipitation. Age hardening is a commonly used method of studying precipitation phenomena in aluminium alloys. While the age hardening curves normally show the evolution of hardness with time at one temperature, the hardness variation after a fixed time at different temperatures (from 120 ^oC to 180 ^oC) is often governed by an activation energy, with the relationship $\Delta HV=\Delta HV_0 \exp(-Q/RT)$,where ΔHV is the hardness variation from one state to other state at temperatureT(in ^oK), ΔHV_0 is the constant term, Q is the activation energy andR is the gas constant [26].

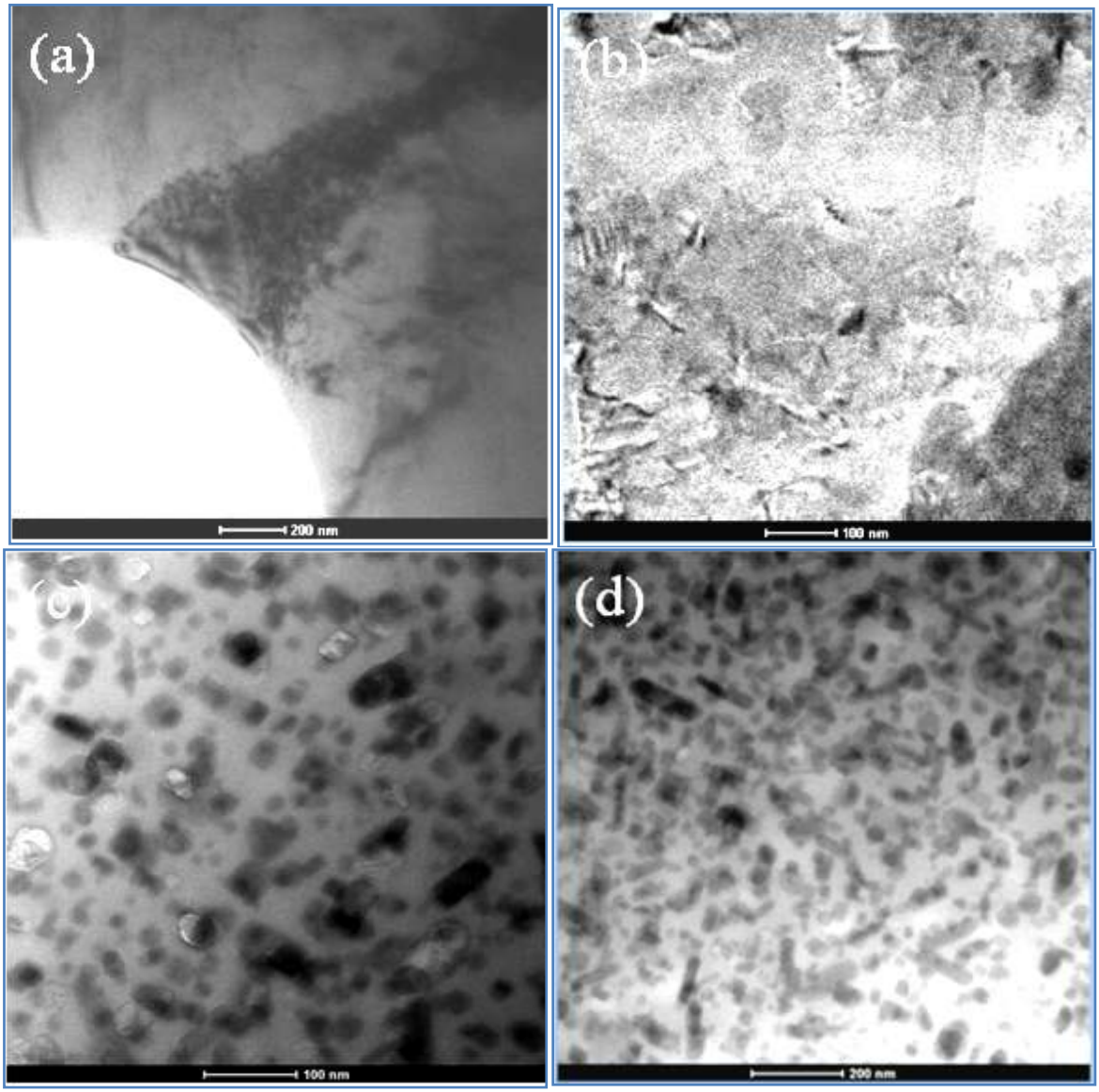

Fig.-7: Illustration of TEM micrographs of as-cast condition (a) Alloy-2, (b) Alloy-3; T_6 (aged at 140 ^{o}C/6 h) condition (c) Alloy-1, (d) Alloy-2.

The activation energy, Q (kJ/mole) can becalculated baseon ageing temperature and time from the Arrhenius equation. By plotting ln(ΔHV) vs. 1/T, the slope of the linear regression fitting will be –Q/R, and the constant ΔHV_0 can be calculated from the intercept with the vertical axis of the linear regression line.Therefore, the activation energy values can be used to reveal the controlling mechanisms ofthe hardening process, e.g., the diffusion of a particular element. It may be noted that age hardening can be used in quantitatively describing and modelling phase transformation kinetics and evaluating its mechanisms [27].The activation energy values have been found from experimental results which are quite low values indicated that the driving force of the precipitation process slow and due to scandium addition to these alloys enhances the precipitation process [in Table-2]. The DSC curves of the present studied alloys at varying heating rates are shown in Fig.-8(a-c). From Fig.-8(a), three peaks marked with 1, 2, 3 are exothermic peaks, and 1', 2', 3' are endothermic peaks. One also can observe in this curve that by increasing the heating rate or at different heating rates, exothermic and endothermic peaks not much shifted from initial points. At first peak 1 appeared at around 220-230 ^{o}C that is due to the precipitation of η phases with GP-II, for second peak 2 appeared at around 455-460 ^{0}C to 550 ^{0}C (for peak 3). At higher exothermictemperatures started precipitates like T, T' and hightemperature stable phases.

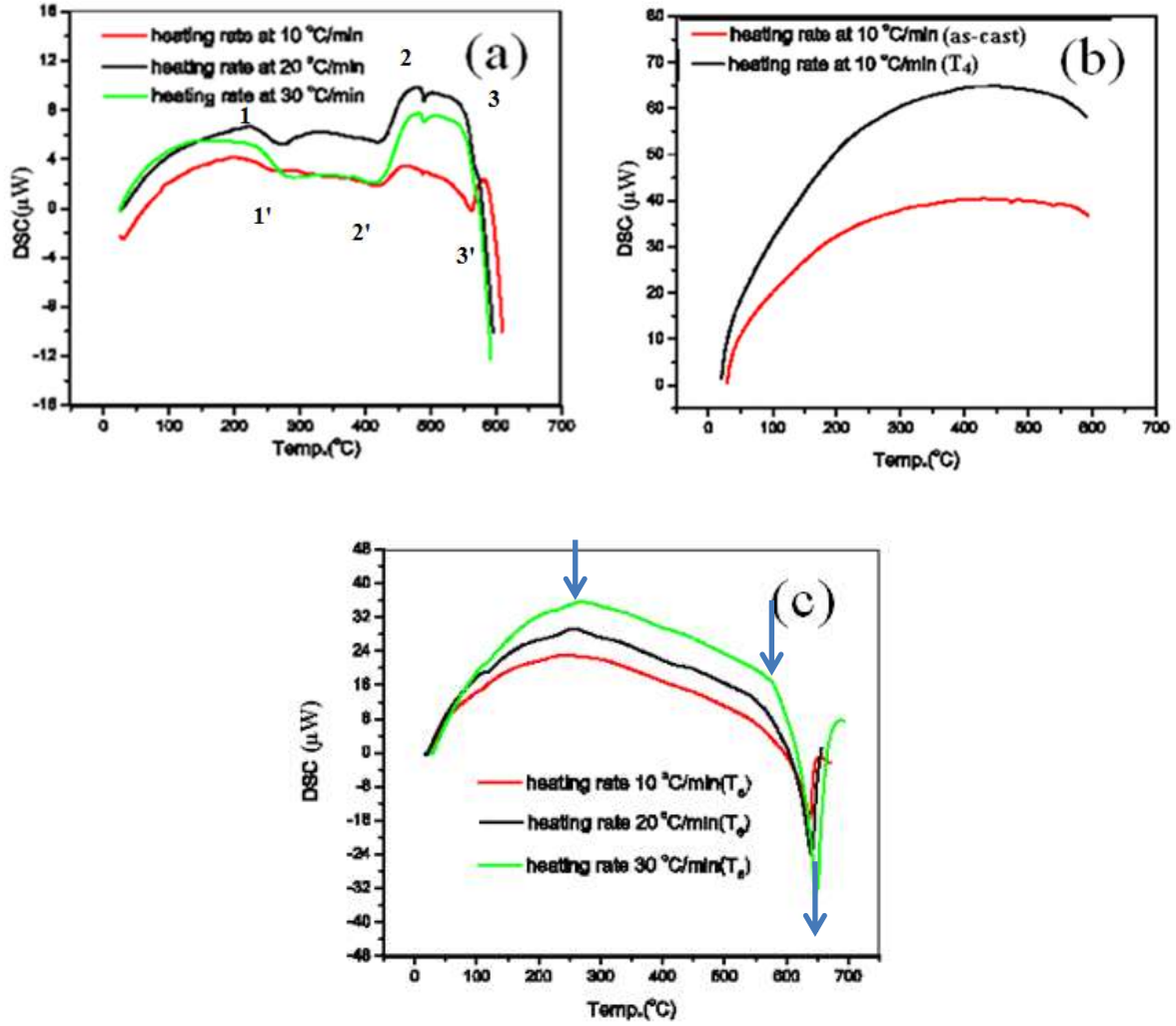

Fig.-8: Illustration of DSC curves at different heating rates (a) Alloy-1(T_6 condition-aged at 140 ^oC/6h); (b) Alloy-2(as-cast and T_4 conditions); (c) Alloy-3 (T_6 condition-aged at 160 ^oC/2h).

Means, at higher temperatures main hardening phases (e.g., GP zones, ή phases) are dissolved rather coarse second phases, coarse microconstituents are formed once peak tends to dissolution mode. From peak 3 started dissolution of precipitates upto around 600 ^oC. The main endothermic peak- 1' appeared at around 270-280 ^oC means dissolution occur of η phases and GP-II zones as continue to peak-2', secondly peak-3' appeared at around 520-530 ^oC, therefore, at this point dissolved all the existing phases (e.g., hardening phases) assumption says from calorimetric studies. From Fig.-8(b) shows at around highest peak exist 410-420 ^oC due to Al_3Sc particles, also this is called exothermic peak in according to calorimetric study.After this point there existing phases are dissolved that is called endothermic mode of phase transition. From Fig.-8(c) shows at around highest peak exist 252-255 ^oC and here most hardeningphases(e.g., ή-phases and Al_3Sc particles) are appeared, and then next transition point comes at around 570 -580 ^oC due to wide range stay from 252 to 580 ^oC varies for effects of Al_3Sc particles and it anti-recrystallization, dispersive effects.Improvements in aluminium alloysfor aerospace applications during the pastfew decades have been associated with an improved understandingofthe relationships among composition, processing,microstructure and properties [28-31**]**.In general, microsturctural features of importance for property control of the aircraft alloy products include-coherency, volume fraction and distribution of strengthening precipitates. These form intentionally during ageing treatments and unintentionally duringquenching. The precipitates normally range in size from 1-10 nm.The ageing orprecipitation heat treatments for aircraft alloy products produce three types of matrix precipitates: GP zones, metastable precipitates and equilibrium precipitates. GP zones are fine, completely coherent clusters of solute elements and have the same crystal structure as the matrix. The GP zones are usually, but not always, theprecursors ofmetastable precipitates.

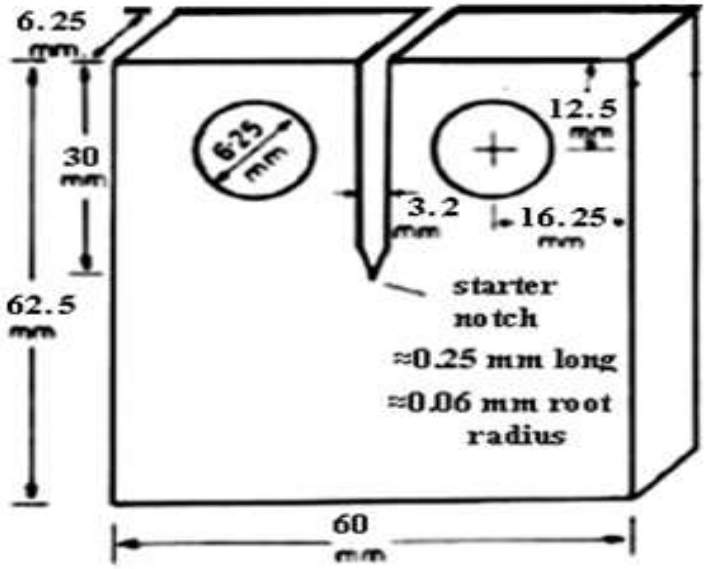

Fig.-9: Design of CT(compact-tension)specimenof fracture toughness test.

The shape and habit plane of the metastable precipitates (the matrix plane on which they precipitate) depend on the balance between strain energy and interfacial free energy. They nucleate primarily in the matrix either homogeneously or heterogeneously at vacancy clusters and less frequently at dislocations. Metastable precipitates normally have a crystal structure which is different from that of the matrix and are completely coherent with the matrix on at least one interface. They have misfit dislocations along interfaces which are not completely coherent. They are larger than GP zones, and often, but not always, form by transformation of a GP zone. They may also nucleate at dislocations, and in Al-alloy systems they prefer to nucleate at these sites. Equilibrium precipitates are larger and more widely spaced. Similarly, size, distribution and coherency of dispersoid particles are also important factors. These form during the ingot preheat by precipitation of the transition elements namely scandium as Al_3Sc particles. They are present by design to control grain structure and degree of recrystallization. Dispersoids normally range in size from 10-200 nm. Because they form from a solid-solid reaction, at least one of their interfaces with the matrix is coherent. The Al_3Sc particles precipitate in a metastable $L1_2$ structure which has a lattice parameter close to that of aluminium and are fully coherent with the matrix. Although the tetragonal form of Al_3Sc is the equilibrium phase, the $L1_2$ structure is remarkably resistant to transformation in the high-strength alloys. Moreover, because of the low diffusion coefficient of scandium in aluminium, the Al_3Sc dispersoids are highly resistance to coarsening. Crystal structure of the others dispersoids (e.g. $Al_{12}Mg_2Cr$, $Al_{12}Mn_3Si$, etc) are non-cubic, larger and less resistant to coarsening at high temperatures. The degree of recrystallization is determined by the thermomechanical history. During bulk metal deformation processing at elevated temperatures, the dislocations in aluminium alloy products arrange into a structure of subgrains by the process known as dynamic recovery. During solution heat treatment, the stored energy of deformation is given an opportunityto decrease by static recovery and/or recrystallization. The tendency for recrystallization is opposed by the Zener drag imposed by the dispersoid particles on migrating boundaries. Zener suggested [32-34] that a grain would cease to grow when its radius, r, divided by the particle volume fraction, f, i.e.: $R_{crit}=(3\beta/4)(r/f)$…….(7), where $\beta\approx1$. Grain size and shape are also controlled by thermomechanical history and may be influenced by the cast grain refining practice. Crystallographic texture is determined by the deformation process used to produce the product and the thermomechanical history. Intermetallic constituent particles form by a liquid-solid eutectic reaction during solidification, primarily from Fe and Si impurities. Because the low solubility of Fe in pure Al is reduced by alloying elements, constituent particles containing Fe are insoluble. Mg_2Si is virtually insoluble in alloys such as 7075. Therefore, the detrimental effect of large constituent phases on the fracture toughness of aluminium alloys. During ageing, heterogeneous precipitation occurs at grain and subgrain boundaries resulting in soft, solute-denuded PFZs in the matrix adjacent to the boundaries. The combination of these soft zones, that can localize strain, and grain boundary precipitates, that can aid in microvoid nucleation, has an adverse effect on fracture toughness. Since Sc particles are small and coherent with the matrix (strong interface), they are usually not involve in the fracture process. As strength increases, ductility and fracture toughness usually decrease. To develop the high toughness the microstructure must accommodate significant plastic deformation, and yet a microstructure that resists plastic deformation is needed high strength. Grain size and degree of recrystallization can have a significant effect on fracture toughness. The desired degree of recrystallization depends on product thickness. i.e., whether

the part is under plane stress or plane strain. In thin products under plane stress, fracture is controlled by plasticity and a small recrystallized grain size is preferable. If the grain size is small enough, plasticity will be enhanced without detrimental, low energy, intergranular fracture. However, for thick products under plane strain, fracture isusually controlled by toughness. Since Sc particles are small and coherentwith the matrix(strong interface),they are usuallynot involve in the fracture process. As strength increases, ductility and

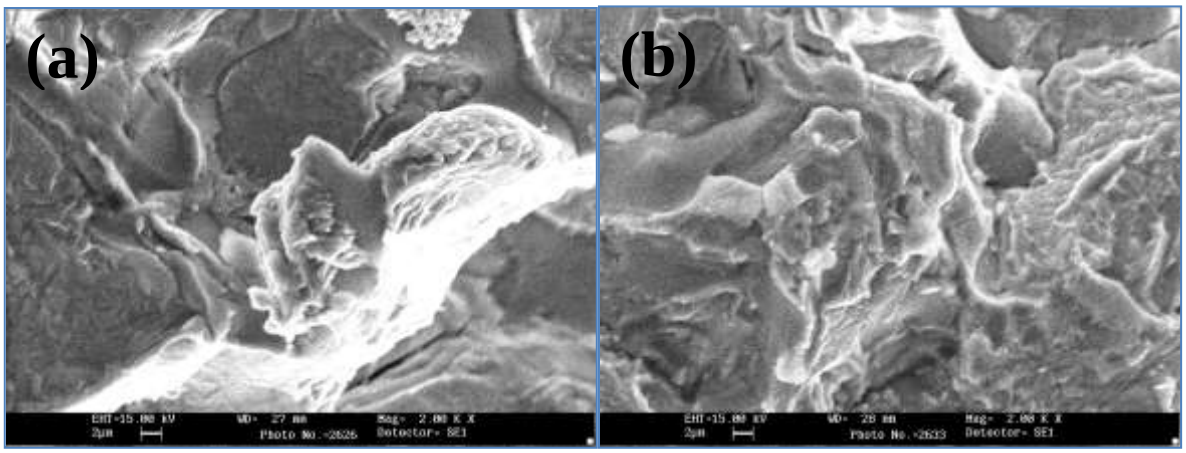

Fig.-10: SEM fractographs of CT specimen (a) Alloy-1, (b) Alloy-2.

fracture toughness usually decrease. To develop the high toughness the microstructure must accommodate significant plastic deformation, and yet a microstructure that resists plastic deformation is needed high strength. Grain size and degree of recrystallization can have a significant effect on fracture toughness. The desired degree of recrystallization depends on product thickness. i.e., whether the part is under plane stress or plane strain. In thin products under plane stress, fracture is controlled by plasticity and a small recrystallized grain size is preferable. If the grain size is small enough, plasticity will be enhanced without detrimental, low energy, intergranular fracture. However, for thick products under plane strain, fracture is usually controlled by coarse particles and an unrecrystallized grain structure is preferable. Aluminium alloy structures loaded below the yield strength, σ_y, or plane strain fracture toughness, K_{IC} may still experience catastrophic failure, even if the load is not cyclic in nature. Cracks may initiate and propagate in the presence of tensile stresses and an aggressive environment.As per D. Duont et al. a model is proposed [35], which predicts the toughness of 7000 series aluminium alloys in a variety of situations, including alloy compositions, different quench rates from the solution treatment temperature and ageing states from underaged to overaged. According to Hahn and Rosenfield models have yielded the dependence of fracture toughness on the volume fraction of second phase particles $K_{IC} \propto f_v^{1/6}$. Another approach, by Garettand Knott, refined by Chen and Knott has aimed to describe the fracture toughness in terms of a critical strain to failure at the crack tip, associated with a critical opening displacement (COD) related to the fracture of second phase particles. This analysis yielded, at constant second phase particle distribution, to a dependence of the fracture toughness with the plasticproperties of the materials (yield stress σ_y, hardening exponent n), and some characteristics of the intermetallic particles (decohesion stress σ_c, spacing λ): $K_{IC} \propto n\sqrt{\sigma_y \sigma_c \lambda}$ ……(8). In the present experimental work has been conducted for both the as-cast aluminiumalloysexhibit valid ASTM K_{IC} (fracture toughness) valuesbased on LEFM(linearelastic fracture mechanics)considerations [36].The testing parameters have been presentedand tabulated in Table-3. We have evaluated cast K_{IC} values in plane strain condition [as per design in Fig.-9] but experimental valuesare marginally lower due to cast inhomogeneties and high volume percentages of porosities and residual elements are major drawbacks for lower K_{IC} values (in Table-3). Form Fig.-10(a-b), shows the typical type of compact-tension fracture surfaces at no scandium addition (for Alloy-1) and with scandium additions (for Alloy-2), respectively. Form the above fracture surfaces could be assumed finer gains obtain for Alloy-2 due to scandium additions. For the Alloy-1[in Fig.-10(a)], decohesion and fracture of the residual second phase appears at the fracture surface. On the other hand, cast solidified grains and microcracks generation at grain boundaries region are appeared visible at the fracture surface. During deformation, some voids generally form on the interfaces between the residual phases and the matrix. For the Alloy-2 [in Fig.-10(b)], indicates a prevailing of intergranular fracture. During deformation, some voids and microcracks are generally formed on the gain boundary regions. In reality, scandium additions not favourable for better toughness due to cast inhomogeneities domination. As the plastic deformation proceeds, residual phases, porosities, coarse second phases and voids are major propagation paths for the cracks. Rather, it may be concluded that the fracture toughness seriously

impaired by grain boundary segregation and porosity of cast alloys. So far, for three alloys have been evaluated tensile properties under T_4 and T_6 conditions [in Table-4]. In as-cast condition tensile properties are not much enhanced due to cast grains inhomogeneties, porosities, grain boundaries segregation and for light weight materials. But for both heat treated conditions for Alloy-2 and Alloy-3 with scandium additions grains refine during solidification, subsequently eliminated cast irregularity with fine dispersions of Al_3Sc particles to anti-recrystallization exhibitor [37]. During solution treatment tensile properties are marginally down due to re-dissolved residual phases and dissolution of grain boundaries segregation and recrystallizedcoarse solidified grains. Present studied alloys in a supersaturated solid solution after casting, scandium elements precipitate into fine coherent Al_3Sc particles during subsequent heat treatment and contribute to increased strength. In addition, the most important strengthening mechanisms of scandium in aged Al-Zn-Mg alloys were Orowan strengthening of secondary Al_3Sc particles.

Table-2: Activation energies, Q (kJ/mole)calculation based on ageing temperature and time from the Arrhenius equation.

Alloy no.	Values of activation energies, Q (±kJ/mole); at ageing time (h)				
	0.5 h	2 h	6 h	10 h	16 h
1	1.70	0.17	0.40	0.89	1.83
2	3.50	5.99	4.65	7.42	6.79
3	1.70	0.80	3.49	3.10	3.58

Table-3: The following parameters have been selected during fracture toughness (K_{IC}) test with standard (ASTM E399) CT specimen with static loading condition.

Alloy nos.	Alloy condition	Experimental parameters								
		Applied load (in N) varies	R ratio	YS (MPa)	UTS (MPa)	Y. Modulus (MPa)	Frequency (f) (Hz)	Numbers of cycles have yielded during pre-crack stage	Crack length Generated (mm)	K_{IC} Values (MPa√m)
1	as-cast and Sc free	1000 to 1700	0.1	80 to 90	175 to 200	3×10^6	1 to 5	130000	0.950	4.54
2	as-cast and with Sc addition	1500	0.1	125	250	6×10^6	5	43000 (sample has broken during pre-crack stage)	-	-
2	as-cast and with Sc addition	1500	0.1	125	250	6×10^6	5	45000	0.554	3.68

Table-4: Results of mechanical properties and fracture toughness values have been tabulated.

Alloy no.	As-cast condition			At different heat treatment conditions				As-cast condition	
	$\sigma_{0.2}$ (MPa)	σ_u (MPa)	δ (%)	$\sigma_{0.2}$ (MPa)	σ_u (MPa)	δ (%)	T_4/T_6	K_{IC} (MPa√m)	Porosity in vol.%
1	50.5	180.7	2.33	48.5	170.6	3.30	T_4	4.54	10.9
2	154.4	249.4	1.93	145.3	234.4	2.22	T_4	3.68	3.33
3	288.0	294.2	3.95	355.0	444.7	3.58	T_6	-	9.86

N.B: yield strength denoted at 0.2% offset from stress-strain curve.

IV. CONCLUSIONS

1. The aluminum alloys have been cast through foundry route. Subsequently, scandium additions enhanced overall mechanical properties through grain refinement mechanisms. Thus, scandium has unique property to modify cast aluminum structure.
2. The optical micrographs revealed cast morphology of virgin aluminiumalloys.

3. The age hardening mechanisms evaluated through Vicker's hardness measurement at 120 ^{o}C, 140 ^{o}C and 180 ^{o}C artificial ageing temperatures. Since age hardening phenomena is function of temperature and time with chemical compositional effects. The Zn:Mg ratios varies lot of transition phases on the basis of with kinetics energy on precipitation.
4. The TEM micrographs revealed for aged alloys (at 140 ^{o}C/6h) as well as artificial ageing treatments supports as small round clusters are typically GP zones, whereas the fine platelet precipitates are the ή phase precipitates, a good resemblance is obtained if we consider that the Zn/Mg ratios of the precipitates compositions are 2.38, and ~1.82-1.83, which are close to 2 for ή($MgZn_2$) and T($Al_2Zn_3Mg_3$)formers, respectively.
5. There are several characterization has been done namely DSC, SEM and FESEM to reveal cast morphology of aluminium alloys.
6. There are several characterizations have been done on cast alloys. The mechanical properties namely tensile (0.2% proof stress, ultimate tensile stress and ductility) and fracture toughness (K_{IC}) properties have been evaluated. At present experimental results have indicated that an increase in impurities (e.g. inform of coarse inclusions), more coarse microconstituents, and more volume percentages of porosity will degrade the fracture toughness of cast aluminum alloys.
7. The maximum benefit from scandium additions in aluminum alloys can be obtained by producing a supersaturated solid solution of solute elements during casting, which is then decomposed during controlled ageing treatments to produce a high number density of fine Al_3Sc dispersoids.
8. There are several theoretical models have been discussed on fundamental aspect on strengthening mechanisms and nucleation of precipitation on grain-refinement principle.
9. Since, Al-Zn-Mg alloys are age hardening or precipitation hardening former to achieved higher strength and it has occurred several phase transition media, which has been shown several theoretical models to clarify insight precipitation kinetics mechanisms. Consequently, Zn:Mg ratios have effective role during precipitation behaviour, phase diagrams as well as various properties of 7000 series aluminum alloys are investigated by J. Yu and his co-worker [2011]by using software package JmatPro.
10. There are several theoretical models have been discussed namely Cahn and Hilliard model is called GP zones model, Hahn and Rosenfield models on fracture toughness properties,H. Yan-hui et al. has been explained on Kampmann and Wagner (KW) type numerical based on precipitation kinetics models, N. Kamp et al. has been explained on both homogeneous and heterogeneous precipitation behavoiur in 7xxx alloys and their transition phases from ή to η phases. In our conclusion has been drawn a good agreement between the model predictions and experimental results on studied alloys.

REFERENCES

[1]. R. Ferragut, A. Somoza, A. Dupasquier, On the two-step ageing of a commercial Al-Zn-Mg alloy; a study by positron lifetime spectroscopy, *Journal of Physics: Condensed Matter, Vol.8* (1996) 8945-8952.

[2]. S.V. Emani, J. Benedyk, P. Nash, D. Chen, Double ageing and thermomechanical heat treatment of AA7075 aluminium alloy extrusions, *Journal of Materials Science, Vol. 44*, 2009, 6384-6391.

[3]. J.H. Kim, J.T. Yeom, J.K. Hong, S.Y. Shim, S.G. Lim, N.K. Park, Effect of Scandium on the Hot extrudability of 7075 Aluminium Alloy, *Metals and Materials International, Vol. 16, No. 4 (2010)*, 669-677.

[4]. S. Costa, H. Puga, J. Barbosa, A.M.P. Pinto, The effect of Sc addition on the microstructure and age hardening behaviour of as cast Al-Sc alloys, *Materials and Design*, *42*(2012), 347-352.

[5]. A. Dupasquier, R. Ferragut, M.M. Iglesias, C.E. Macchi, M. Massazza, P. Mengucci, G. Riontino, A. Somoza, Early solute clustering in an AlZnMg alloy, *Materials Science Forum, Vols. 445-446* (2004), 16-20.

[6]. P.K. Mandal, P.K. Ghosh, Development of high strength Al-Zn-Mg alloys for automotive application, *Indian Foundry Journal, Vol. 60, No. 4*, April 2014, 32-39.

[7]. Z. Ahmed, The properties and Application of Scandium-Reinforced Aluminium, *Journal of the Minerals, Metals and Materials Society (JOM), Vol. 55, Issue 2*, February 2003, 35-39.

[8]. T. Ungar, J. Lendvai, I. Kovacs, G. Groma, E. Kovacs-Csetenyi, The decomposition of solid solution state in the temperature range 20 to 200 ^{o}C in an Al-Zn-Mg alloy, *Journal of Materials Science 14*, 1979, 671-679.

[9]. G. Cacciamani, P. Riani, G. Borzone, N. Parodi, A. Saccone, R. Ferro, A. Pisch, R. Schmid-Fetzer, Thermodynamic measurements and assessment of the Al-Sc system, *Intermetallics 7* (1999), 101-108.

[10]. E.A. Starke Jr., J.T. Staley, Application of modern aluminium alloys to aircraft, *Prog. Aerospace Sci. Vol. 32*, 131-172, 1996.

[11]. W.J. Poole, J.A. Saeter, S. Skjervold, G. Waterloo, A Model for Predicting the Effect of Deformation after Solution Treatment on the Subsequent Artificial Aging Behavior of AA7030 and AA7108 Alloys, *Metallurgical and Materials Transactions A, Vol. 31A*, September 2000, 2327-2338.

[12]. P. Leo, E. Cerri, H.J. McQueen, S. Chiozzi, Microstructure and mechanical characterization of an Al-Zn-Mg alloy after various heat treatments and room temperature deformation, *Materials Science Forum, Vols. 604-605* (2009), 67-76.

[13]. J.C. Werenskiold, A. Deschamps, Y. Brechet, Characterization and modeling of precipitation kinetics in an Al-Zn-Mg alloy, *Materials Science and Engineering A293* (2000), 267-274.
[14]. J. Yu, X. Li, Modelling of the Precipitated Phases and Properties of Al-Zn-Mg-Cu Alloys, *Journal of Phase Equilibria and Diffusion, Vol. 32, No. 4*, 2011, 350-360.
[15]. Dr. Eng. A.H. Ataiwi, "Thermo mechanical Treatments of Variables percentage of Al-Zn-Mg alloys", *Engg. and Technoogy Journal, University of Technology, Vol. 25, No. 7*, 2007.
[16]. R. Ferragut, A. Somaza, A. Tottley, A. Torriani, Precipitation kinetics in Al-Zn-Mg commercial alloys, *Jr. of Materials Processing and Technology 141*, 2003, 35-40.
[17]. G. Liu, G.J. Zhang, X.D. Ding, J. Sun, K.H. Chen, Modeling the strengthening response to aging process of heat-treatable aluminium alloys containing plate/disc- or rod/needle-shaped precipitates, *Materials Science and Engineering A344* (2003) 113-124.
[18]. T. Hu, K. Ma, T.D. Topping, J.M. Schoenung, E.J. Lavernia, Precipitation phenomena in an ultrafine-grained Al alloy, *Acta Materialia 61* (2013), 2163-2178.
[19]. Y. Jing, C. Li, Z. Du, F. Wang, Y. Song, The thermodynamics analysis of Guinier-Preston zones in aged supersaturated Al-Cu alloys, *Computer Coupling of Phase Diagrams and Thermochemistry Vol. 32, Issue 1*, March 2008, 164-170.
[20]. H. Yan-hui, G. Yan-x, L. Zhiyi, L. Yun-tao, C. Xu, Modelling of whole process of ageing precipitation and strengthening in Al-Cu-Mg-Ag alloys with high Cu-to-Mg mass ratio, *Transaction of Nonferrous Metals Society of China 20, 5*, 2010, 863-869.
[21]. N. Kamp, A. Sullivan, R. Tomasi, J.D. Robson, Modelling heterogeneous precipitation in 7xxx aluminium alloys during complex processing, *Materials Science Forum, Vols. 519-521* (2006) pp. 1435-1440.
[22]. N.M. Han, X.M. Zhang, S.D. Liu, D.G. He, R. Zhang, Effect of solution treatment on the strength and fracture toughness of aluminium alloy 7050, *Journal of Alloys and Compounds 509* (2011) 4138-4145.
[23]. X.M. Li, M.J. Starink, DSC Study on Phase Transitions and Their Correlation with Properties of Overaged Al-Zn-Mg-Cu Alloys, *Journal of Materials Engineering and Performance, Vol. 21(6)*, June 2012, pp. 977-984.
[24]. E. Salamci, Calorimetric and transmission electron microscopy studies of spray deposited Al-Zn-Mg-Cu alloys, *Materials Science and Technology, Vol. 20, July 2004,* pp. 859-863.
[25]. Y. Deng, Z. Yin, K. Zhao, J. Duan, Z. He, Effects of Sc and Zr microalloying additions on the microstructure and mechanical properties of new Al-Zn-Mg alloys, *Journal of Alloys and Compounds 530*, 2012, 71-80.
[26]. W. Sha, Activation energy for precipitation hardening and softening in aluminium alloys calculated using hardness and resistivity data, *Physica Status Solidi (a) 203, No. 8*, 2006, 1927-1933.
[27]. W. Sha, Application of simple practical models for early stage ageing precipitation kinetics and hardening in aluminium and magnesium composites, *Materials and Design 28, Issue 5*, 2007, 1524-1530.
[28]. A.K. Noor, S.L. Venneri, D.B. Paul, M.A. Hopkins, Structures technology for future aerospace systems, *Computers and Structures 74* (2000), 507-519.
[29]. J.S. Santner, D. Eylon, Fatigue Behaviour and Failure Mechanisms of Modified 7075 Aluminium Alloys, *Metallurgical Transactions A, Vol. 10A*, July 1979, 841-848.
[30]. J.C. Williams, E.A. Starke, Jr., Progress in structural materials for aerospace systems, *Acta Materialia 51* (2003) 5775-5799.
[31]. A. Heinz, A. Haszler, C. Keidel, S. Moldenhauer, R. Benedictus, W.S. Miller, Recent development in aluminium alloys for aerospace applications, *Materials Science and Engineering A 280* (2000) 102-107.
[32]. K. Ihara, Y. Miura, Dynamic recrystallization in Al-Mg-Sc alloys, *Materials Science and Engineering A 387-389* (2004), 647-650.
[33]. J. Royset, N. Ryum, Scandium in aluminium alloys, *International Materials Reviews, Vo. 50, No. 1*, 2005, 19-44.
[34]. H. Loffler, I. Kovacs, J. Lendvai, Decomposition processes in Al-Zn-Mg alloys, *Journal of Materials Science, 18* (1983), 2215-2240.
[35]. D. Dumont, A. Deschamps, Y. Brechet, A model for predicting fracture mode and toughness in 7000 series aluminium alloys, *Acta Materialia 52, Issue 9*, 17 May 2004, 2529-2540.
[36]. K.H.W. Seah, S.C. Sharma, Fracture toughness of cast Al-Zn-Mg alloys, *Journal of Materials Science and Technology, Vol. 12*, pp. 199-202, 1996.
[37]. S.V. Senkova, O.N. Senkova, D.B. Miracle**,** Cryogenic and Elevated Temperature Strengths of an Al-Zn-Mg-Cu Alloy Modified with Sc and Zr, *Metallurgical and Materials Transactions A, Vol. 37A*, December 2006, 3569-3575.